5766–5774 Nucleic Acids Research, 2012, Vol. 40, No. 12 Published online 1 March 2012
doi:10.1093/nar/gks208

Raman spectroscopic detection of the T-Hg^{II}-T base pair and the ionic characteristics of mercury

Tomomi Uchiyama[1,2], Takashi Miura[2], Hideo Takeuchi[2], Takenori Dairaku[1], Tomoyuki Komuro[1,2], Takuya Kawamura[1], Yoshinori Kondo[1], Ladislav Benda[3], Vladimír Sychrovský[3,*], Petr Bouř[3], Itaru Okamoto[4,*], Akira Ono[4] and Yoshiyuki Tanaka[1,*]

[1]Laboratory of Molecular Transformation, [2]Laboratory of Bio-Structural Chemistry, Graduate School of Pharmaceutical Sciences, Tohoku University, 6-3 Aza-Aoba, Aramaki, Aoba-ku, Sendai, Miyagi 980-8578, Japan, [3]Department of Molecular Spectroscopy, Institute of Organic Chemistry and Biochemistry, Academy of Sciences of the Czech Republic, Flemingovo nám. 2, 16610, Praha 6, Czech Republic and [4]Department of Material and Life Chemistry, Faculty of Engineering, Kangawa University, 3-27-1 Rokkakubashi, Kanagawa, Yokohama, Kanagawa-ken 221-8686, Japan

Received January 10, 2012; Revised February 15, 2012; Accepted February 16, 2012

ABSTRACT

Developing applications for metal-mediated base pairs (metallo-base-pair) has recently become a high-priority area in nucleic acid research, and physicochemical analyses are important for designing and fine-tuning molecular devices using metallo-base-pairs. In this study, we characterized the Hg^{II}-mediated T-T (T-Hg^{II}-T) base pair by Raman spectroscopy, which revealed the unique physical and chemical properties of Hg^{II}. A characteristic Raman marker band at 1586 cm^{-1} was observed and assigned to the C4=O4 stretching mode. We confirmed the assignment by the isotopic shift (^{18}O-labeling at O4) and density functional theory (DFT) calculations. The unusually low wavenumber of the C4=O4 stretching suggested that the bond order of the C4=O4 bond reduced from its canonical value. This reduction of the bond order can be explained if the enolate-like structure (N3=C4-O4^{-}) is involved as a resonance contributor in the thymine ring of the T-Hg^{II}-T pair. This resonance includes the N-Hg^{II}-bonded state (Hg^{II}-N3-C4=O4) and the N-Hg^{II}-dissociated state (Hg^{II+} N3=C4-O4^{-}), and the latter contributor reduced the bond order of N-Hg^{II}. Consequently, the Hg^{II} nucleus in the T-Hg^{II}-T pair exhibited a cationic character. Natural bond orbital (NBO) analysis supports the interpretations of the Raman experiments.

INTRODUCTION

Metal-mediated nucleic acid base pairs are extensively studied molecules that are of interest because of their ability to expand the genetic code and provide new materials for nano-devices (1–15). These artificial base pairs can be made by substituting the natural nucleobases with a planar metal chelator in the DNA molecule (1–15). As an alternative, our group discovered that even the natural base, thymine, can form a stable mercury^{II}-mediated T-T base pair (T-Hg^{II}-T pair) (16–22). The RNA analogue of this molecule (U-Hg^{II}-U) also exists as a stable complex (23–25). The metal-mediated base pairs can only form with Hg^{II}, and they are used in many types of Hg^{II}-sensor (16,26–30). The DNA molecule itself has potential as a component of future nano-devices, and the introduction of a T-Hg^{II}-T pair into the sequence could enable the physical and chemical properties of such materials to be fine-tuned (31–33).

Although the T-Hg^{II}-T pair has been extensively studied since 2004 (16,17,26–33), its precise chemical structure was only revealed by ^{15}N NMR spectroscopy in 2007 (20–22). In the NMR analysis, the thymine was ^{15}N-labeled at N3 and incorporated into the DNA duplex **1•2**: d(CGCGTT GTCC) • d(GGACTTCGCG) (Figure 1). In the presence of the Hg^{II} ion, the thymine residues formed a T-Hg^{II}-T pair, and ^{15}N–^{15}N *J*-coupling across Hg^{II} ($^{2}J_{NN}$) was detected (Figure 1c), which provided unambiguous evidence of the formation of the N3-Hg^{II}-N3 bond in the T-Hg^{II}-T pair (20–22). This *J*-coupling value was theoretically examined by density functional theory (DFT)

*To whom correspondence should be addressed. Tel: +420 220183234; Fax: +420 220183578; Email: vladimir.sychrovsky@uochb.cas.cz
Correspondence may also be addressed to Itaru Okamoto. Tel: +81 45 481 5661 (ext 3901); Email: i-okamoto@kanagawa-u.ac.jp
Correspondence may also be addressed to Yoshiyuki Tanaka. Tel:/Fax: +81 22 795 5917; Email: tanaka@mail.pharm.tohoku.ac.jp

The authors wish it to be known that, in their opinion, the first two authors should be regarded as joint First Authors.

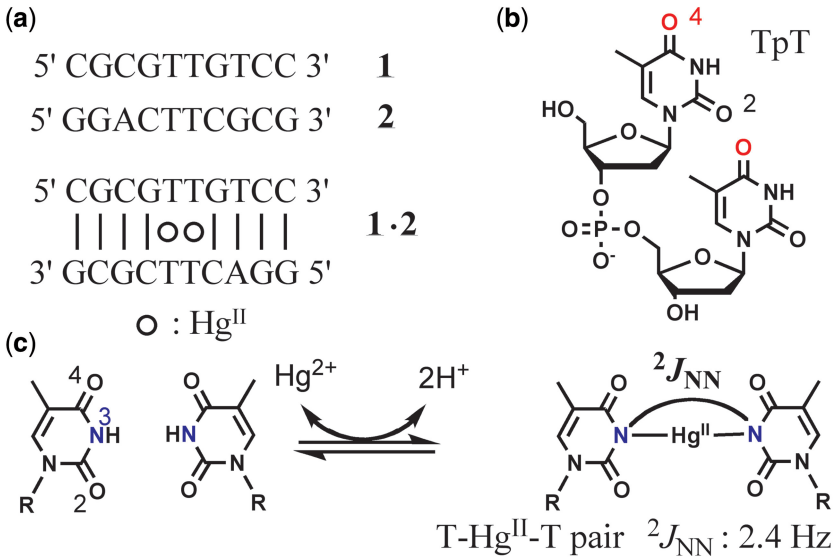

Figure 1. Sequences of DNA oligomers and the structure of the T-Hg^{II}-T pair. (**a**) The sequences of the DNA oligomers used for the NMR and Raman spectral measurements. (**b**) Chemical structure of thymidylyl (3′–5′) thymidine (TpT). The numbering of each carbonyl oxygens is indicated and the labeled oxygen atoms in ^{18}O-labeled TpT are colored in red. (**c**) The reaction scheme for the T-Hg^{II}-T pair formation is shown with 2-bond ^{15}N–^{15}N *J*-coupling ($^{2}J_{NN}$). The numbering system for thymine is also shown, and the N3 atom is colored in blue.

calculations (34). Although various data (35–48) hinted at the chemical structure of the T-Hg^{II}-T pair prior to these studies, its chemical structure was conclusively determined by these studies (20–22,34).

However, despite elucidation of the precise chemical structure of the T-Hg^{II}-T base pair, the nature of the mercury atom in the base pair is unclear. To address this, we used Raman spectroscopy to measure the spectra of the T-Hg^{II}-T pair under different conditions. In the Raman spectra, we identified characteristic bands that were sensitive to irregular base-pair linkage that we assigned using site-specific ^{18}O-labeling. These bands could also be interpreted using DFT calculations. Our analysis revealed several interesting properties of the N-Hg^{II} bonds, e.g. the bond order by natural bond orbital (NBO) analysis.

MATERIALS AND METHODS

DNA synthesis

DNA oligomers (CGCGTTGTCC **1** and GGACTTCGC G **2**) and non-labeled thymidylyl (3′–5′) thymidine (TpT) were synthesized by the phosphoramidite method (Figure 1a and b), and purified using a reversed-phase column (COSMOSIL 5C18-AR-300; Nakalai Tesque, Kyoto, Japan). The solutions containing non-labeled TpT were evaporated under vacuum several times to remove unwanted triethylammonium acetate buffer and acetonitrile. The DNA oligomers **1** and **2** were further purified using an anion-exchange column (UNO Q-6; BIO-RAD, CA, USA) to exchange the triethylammonium counter ion with sodium. Excess NaCl was removed using a gel filtration column (TSK-GEL G3000PW; TOSOH, Tokyo, Japan) with MILLI-Q water (MILLIPORE, MA, USA) as the mobile phase. Each oligomer was quantitated by UV absorbance at 260 nm after digestion with nuclease P1 (Yamasa, Choshi, Japan). $Hg(ClO_4)_2$ (Wako, Osaka, Japan) was used as the Hg^{II} source. ^{18}O-labeled TpT at the O4 position (^{18}O4-labeled TpT) was synthesized by the procedure shown in Supplementary Scheme S1; further details are described in the Supplementary Data.

Raman spectroscopy

To prepare the Hg^{II}-DNA complex, a solution of 2.0 mM DNA duplex **1•2** and 4.8 mM $Hg(ClO_4)_2$ were made, and excess Hg^{II} cations were removed using a chelating resin (Chelex 100, BIO-RAD) as described previously (20). The resulting solution was concentrated to yield the Hg^{II}-DNA complex at a final concentration of 2.0 mM for measurement purposes. To prepare the Hg^{II}-free DNA duplex, $NaClO_4$ was added to the 2.0 mM DNA duplex **1•2** solution to enable the final concentration of the ClO_4^- ion to be adjusted to 9.6 mM.

The Raman spectra of TpT were recorded using a 10 mM TpT solution containing 0–1.75 molar equivalents of $Hg(ClO_4)_2$ as a simple model for the system. The pH of the solution was adjusted to 6.5 by direct titration with HCl or NaOH. The Raman spectra of thymidine 5′-monophosphate (5′-TMP) were recorded under various conditions. Each sample was sealed in a glass capillary and excited with the 514.5 nm line of a Coherent Innova 70 Ar^+ laser. The Raman scattered light was collected with a camera lens, dispersed on a Jasco NR-1800 triple spectrometer, and detected with a liquid-nitrogen-cooled CCD detector. The temperatures of the samples were maintained at 295 K. Raman scattering from the solvent was subtracted from each spectrum.

DFT calculations

The geometry of 1-methylthymine, and two possible patterns of the T-Hg^{II}-T complexes (Supplementary Figure S1) were optimized by Gaussian 03, rev. D02 (49) at the B3LYP/6-31+G(d,p) level of theory with the polarizable continuum model (PCM) of water solvent. The core electrons of the mercury atom were treated using the MWB60 relativistic pseudo-potential, while the valence electrons were treated using the MWB60 basis set. For fully optimized structures, vibrational analysis was performed and the back-scattered Raman intensities were calculated at the same level of theory. The calculated line spectra were weighted by the temperature factor (50,51) and convoluted with Lorentzian band shapes, using 5 cm^{-1} full width at half height. ^{18}O isotope effects were evaluated using the same force field and different oxygen masses.

The two possible topologies of the T-Hg^{II}-T complex shown in Supplementary Figure S1a and b produced almost the same spectra (Supplementary Figure S2), and the topology shown in Supplementary Figure S1a was used for comparison with experiment. Natural charges and bond orders were calculated at the B3LYP/6-31+G(d,p)/PCM(water) level with the NBO 5.0 program linked to Gaussian (49).

NMR spectra of duplex 1•2 and TpT

For the DNA duplex **1•2**, 1D ^{1}H NMR spectra were recorded as Hg^{II}-free, Hg^{II}-bound and Hg^{II}-removed forms. We found that the Hg^{II} atoms can be removed even at temperatures below 100°C (Supplementary Figure S3). NMR spectra were also recorded for TpT to verify the complex formation of TpT with Hg^{II} (Supplementary Figures S4 and S5), and the T-Hg^{II}-T pair formations were confirmed(Supplementary Figures S3–S5).

RESULTS

Raman spectroscopic characterizations of the T-Hg^{II}-T pair

The Raman spectra of the DNA duplex **1•2** in the presence and absence of $Hg(ClO_4)_2$, are shown in Figure 2. Many small changes were observed in the duplex, in particular, those at 1704, 1576, 1487, 1422, 1372, 1172 and 749 cm^{-1}, caused by the complexation with Hg^{II}. In previous NMR studies (20–22), we confirmed that Hg^{II} exclusively binds to the T-T mismatch sites in the same DNA duplex **1•2** to form two successive T-Hg^{II}-T pairs, based on the observation of 2-bond ^{15}N–^{15}N *J*-coupling (Figure 1). Therefore, we can attribute the observed Raman spectral changes to the same Hg^{II}-binding.

Because the changes in the Raman spectra of the DNA duplex were small and were overlapped by the stronger Raman bands from the sugar-phosphate backbone and bases other than T, we used the Raman spectra of the thymidylyl (3′–5′) thymidine (TpT) for detailed studies. The spectra acquired in the presence and absence of

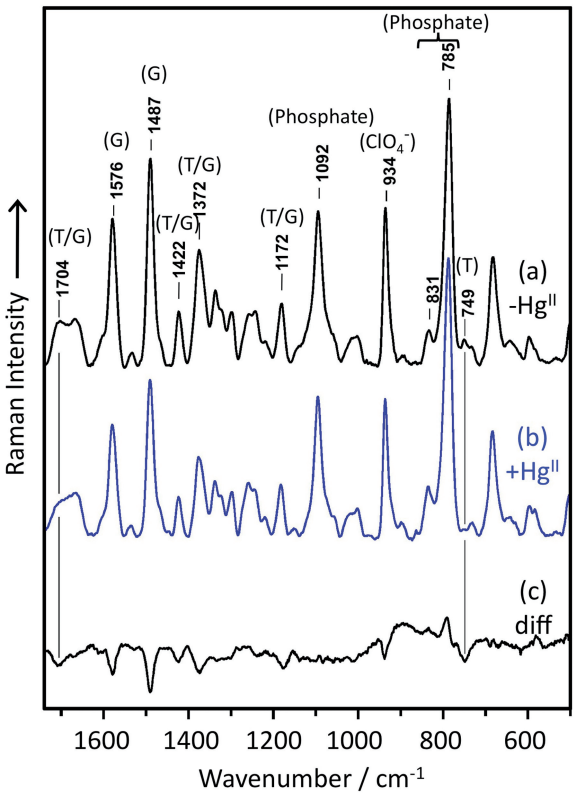

Figure 2. Raman spectra of the duplex **1•2** in the absence (**a**) and presence (**b**) of Hg^{II}, and the difference spectrum [(b)–(a)] (**c**) are shown. In spectrum (b), the molar ratio (Hg^{II}/duplex) was 2.0. Characteristic bands are highlighted with their wavenumber and their main origins. The band at 934 cm^{-1} is due to ClO_4^-. Bands at 785, 831 and 1092 cm^{-1} were mainly due to vibration from the phosphate group. The phosphate Raman band at 1092 cm^{-1} was used as a reference for spectral intensity. Bands at 1487 and 1576 cm^{-1} are mainly due to guanine, and their negative peaks in spectrum (c) may be ascribed to an increase in the stacking interaction of guanosine residues upon the formation of the T-Hg^{II}-T base pair.

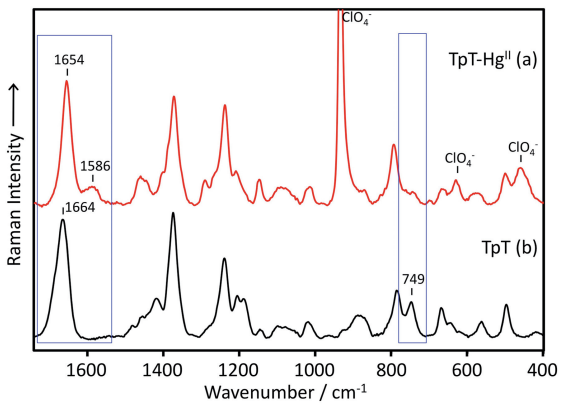

Figure 3. Raman spectra of TpT in the presence (Hg^{II}/TpT = 1.75) (**a**) and absence (**b**) of Hg^{II}. The Raman band at 934 cm^{-1} in the spectrum of the Hg^{II}–TpT complex arises from ClO_4^-.

$Hg(ClO_4)_2$ are shown in Figure 3. Clearly, the bands present at 1664 and 749 cm^{-1} were significantly affected by the addition of $Hg(ClO_4)_2$, which is consistent with the duplex results.

Raman band at 749 cm^{-1}: evidence for the formation of the T-Hg^{II}-T base pair

The Raman band at 749 cm^{-1} was perturbed upon the complexation of thymine with Hg^{II} for both the duplex **1•2** and TpT (Figures 2 and 3). We next investigated the Raman band of TpT and its Hg^{II}-complex in H_2O and D_2O (Figure 4). Upon the addition of Hg^{II} to TpT, the Raman band at 749 cm^{-1} was suppressed (Figure 4c and d). For the Hg^{II}-free TpT in D_2O, it is shifted by 13 cm^{-1} (Figure 4a and b). At this stage, the vibrational mode for the Raman band at 749 cm^{-1} was found to include the contribution from the imino proton of the thymine base. To examine if the imino proton contributed to this band, we recorded the Raman spectra of deprotonated thymidine 5′-monophosphate (5′-TMP) under strong basic conditions. The spectra obtained for 5′-TMP showed that the Raman band at 749 cm^{-1} disappeared under strong basic conditions (Supplementary Figure S6). Thus, its absence upon the addition of Hg^{II} indicates deprotonation of N3 due to the Hg^{II}-binding. Furthermore, the spectral change that occurred at around 749 cm^{-1} in the DNA duplex **1•2** may be similarly explained (Supplementary Figure S7). In summary, we have demonstrated the T-Hg^{II}-T pairing by the Raman spectra.

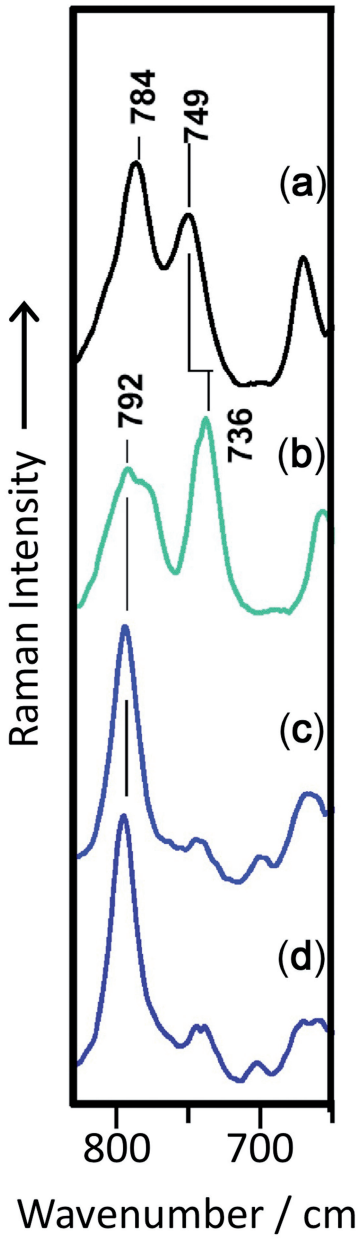

Figure 4. Raman spectra of TpT (650–830 cm^{-1}). (**a**) TpT alone in H_2O. (**b**) TpT alone in D_2O. (**c**) The Hg^{II}–TpT complex in H_2O. (**d**) The Hg^{II}–TpT complex in D_2O.

Raman bands around 1664 cm^{-1} of TpT as a probe for thymine–Hg^{II} interaction

We observed that the Raman bands around 1664 cm^{-1} from TpT altered upon Hg^{II}-binding. As the broad Raman band at 1664 cm^{-1} includes contributions from both the C2=O2 and C4=O4 stretches of thymine (52,53) and these carbonyl groups are in close proximity to Hg^{II}, the Raman spectral features in this region may be useful for probing the thymine-Hg^{II} interactions. To examine the spectral changes around 1664 cm^{-1} in detail, Hg^{II}-titration experiments of TpT were performed (Figure 5). As the concentration of Hg^{II} was increased, a shoulder band at 1685 cm^{-1} lost intensity and a new band at 1586 cm^{-1} emerged (Figure 5). This strongly suggests that at least one or both of the carbonyl groups C2=O2 and C4=O4 in the T-Hg^{II}-T pair were affected by Hg^{II}-binding. In addition, if the newly emerged Raman band at 1586 cm^{-1} is assigned to the stretching mode of the carbonyl groups, it appears that quite a large perturbation occurred to the C=O double bond(s) in thymine upon Hg^{II}-complexation.

Raman spectra of ^{18}O-labeled TpT

To determine which of the C2=O2 and C4=O4 groups of thymine was more affected by the Hg^{II}-complexation, ^{18}O-labeled TpT at the O4 position ($^{18}O4$-labeled TpT) was synthesized (Figure 1b). In Figure 6, the Raman

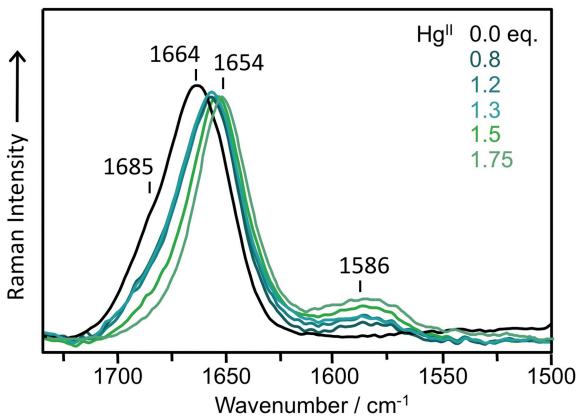

Figure 5. Hg^{II}-titration experiments of TpT by Raman spectroscopy. The molar equivalencies represented by each color are as follows: black: 0.0 eq., indigo: 0.8 eq., blue: 1.2 eq., light blue: 1.3 eq., green: 1.5 eq. and light green: 1.75 eq.

spectra of ^{18}O4-labeled and non-labeled TpT in the presence and absence of $Hg(ClO_4)_2$ are shown, with the main contributions provided by DFT calculations. The 1586 cm^{-1} (non-labeled) band was specifically shifted to 1570 cm^{-1} for the ^{18}O4-labeled TpT (Figure 6), which clearly indicates that the band originates from the vibrational mode associated with the C4=O4 carbonyl group.

DFT calculations of the Raman spectra

To find why the experimental wavenumber of the newly emerged Raman band at 1586 cm^{-1} (TpT) was exceptionally low for a C=O stretching mode, DFT calculations of the Raman spectra for the T-Hg^{II}-T base pair were performed (Figure 7). The DFT calculations reproduced the band at 1586 cm^{-1} (assignment details: Figures 6 and 7). The normal mode analysis also confirms that this band comes from the C4=O4 stretching vibration (Figure 8). A closer look revealed that this band was actually composed of two normal modes (Figure 8), namely, the in-phase and out-of-phase combinations of the C=O stretching vibration of thymine bases in the T-Hg^{II}-T pair. Both modes involve vibration of all carbonyl groups in the T-Hg^{II}-T pair, but the major contribution comes from C4=O4.

The calculated Raman spectra of 1-methylthymine and the T-Hg^{II}-T pair whose O4 atoms were substituted with ^{18}O are also shown in Figure 7a and c. In line with our experimental evidence, the theoretical C4=O4 stretching bands were shifted toward low-wavenumbers (Figure 7c and d).

The shoulder band observed at 1685 cm^{-1} in Hg^{II}-free TpT (non-labeled compound) was assigned to the C2=O2 stretching. Upon ^{18}O4-labeling, this band moved to 1660 cm^{-1} and overlapped with that of the C5=C6 stretching (Figure 6).

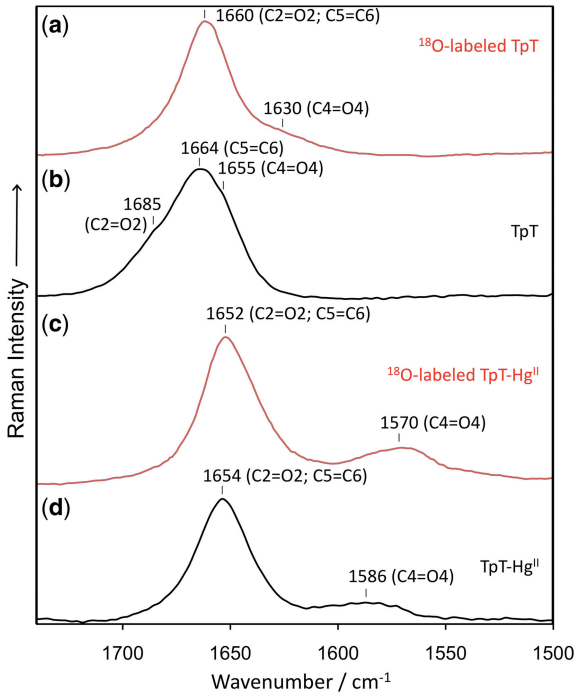

Figure 6. Raman spectra of (**a**) ^{18}O4-labeled TpT, (**b**) TpT, (**c**) ^{18}O4-labeled Hg^{II}–TpT complex (Hg^{II}/TpT = 1.75) and (**d**) Hg^{II}–TpT complex (Hg^{II}/TpT = 1.75). Normal modes for Hg^{II}-free 1-methylthymine (non-labeled and ^{18}O-labeled ones) are shown in Supplementary Figure S10. As a rough assignment based on the theoretical spectra (Figure 7) and the normal mode analyses (Figure 8 and Supplementary Figure S10), the main contributors to the experimental Raman bands around 1664 cm^{-1} were assigned as follows. (a) ^{18}O4-labeled Hg^{II}-free TpT: 1660 cm^{-1} C2=O2 stretching and C5=C6 stretching; 1630 cm^{-1} C4=O4 stretching. (b) Hg^{II}-free TpT: 1685 cm^{-1} C2=O2 stretching; 1664 cm^{-1} C5=C6 stretching; 1655 cm^{-1} C4=O4 stretching. (c) ^{18}O4-labeled Hg^{II}–TpT complex: 1652 cm^{-1} C2=O2 stretching and C5=C6 stretching; 1570 cm^{-1} C4=O4 stretching. (d) Hg^{II}–TpT complex: 1654 cm^{-1} C2=O2 stretching and C5=C6 stretching; 1586 cm^{-1} C4=O4 stretching. The assignment of the Raman bands for Hg^{II}-free TpT was principally the same as in reference (48).

DISCUSSION

Although the wavenumber of 1586 cm^{-1} is exceptionally low for the C4=O4 carbonyl stretching compared to normal carbonyl stretching, the ^{18}O-isotope shift of the Raman bands demonstrated that the main contribution to the characteristic 1586 cm^{-1} band comes from the C4=O4 stretching mode. The DFT calculations further supported this assignment (Figure 8). The band at 1586 cm^{-1} was also observed by Morzyk-Ociepa and Michalska (48), who tentatively assigned it (based on the DFT calculations) using a deprotonated 1-methylthymine anion as a hypothetical model of the T-Hg^{II}-T pair. In contrast, we have simulated the Raman spectra of the T-Hg^{II}-T pair using a more realistic system that includes the heavy metal Hg^{II} (1-methylthymine-Hg^{II} (2:1) complex). Consequently, our DFT calculations further revealed that this band was composed of the collective

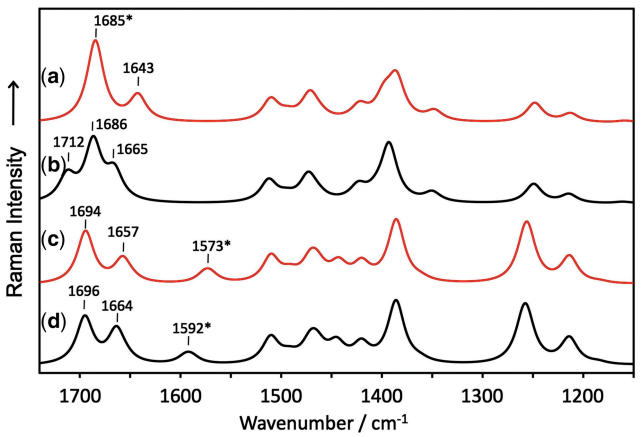

Figure 7. The high-wavenumber range of theoretical Raman spectra. (**a**) ^{18}O4-labeled 1-methylthymine; (**b**) non-labeled 1-methylthymine; (**c**) ^{18}O4-labeled 1-methylthymine–Hg^{II} (2:1) complex; and (**d**) non-labeled 1-methylthymine–Hg^{II} (2:1) complex. Throughout the calculations, 1-methylthymine was used as a model of thymidine. Major contributors to the Raman bands around the C=O stretching region in the theoretical spectra are as follows: (b), 1712 cm^{-1}: C2=O2 stretching; 1686 cm^{-1}: C5=C6 stretching; 1665 cm^{-1}: C4=O4 stretching. (d), 1696 cm^{-1}, C5=C6 stretching; 1664 cm^{-1}, C2=O2 stretching; 1592 cm^{-1} (summation of two C4=O4 stretching modes in Figure 8). Asterisks indicate an apparent wavenumber due to the band overlap.

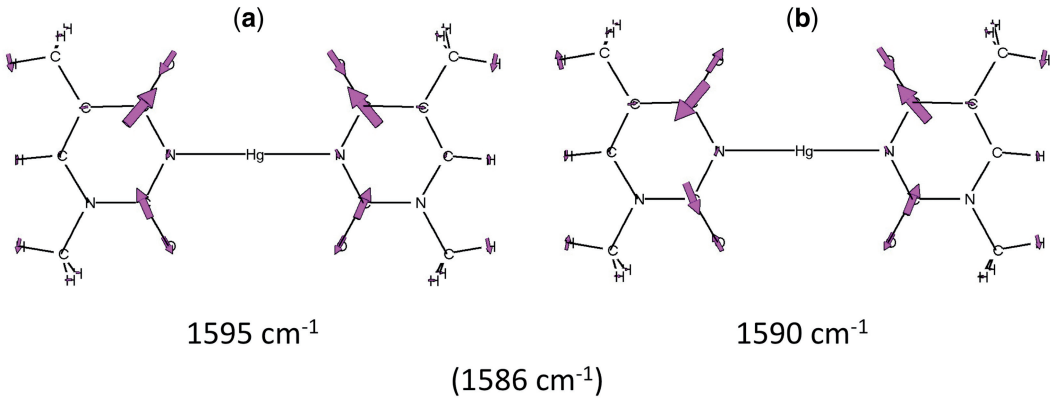

Figure 8. Normal modes for the experimental Raman bands around 1586 cm^{-1} in the T-Hg^{II}-T pair. The theoretical wavenumbers (1595 and 1590 cm^{-1}) are indicated.

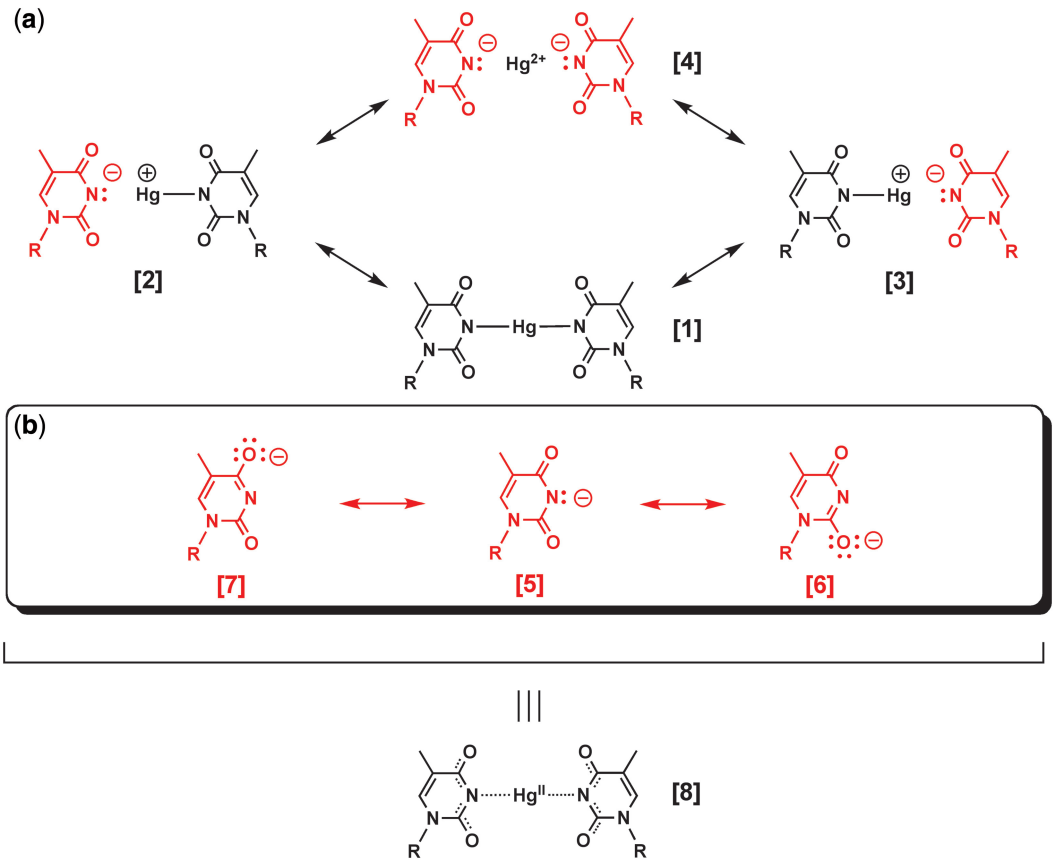

Figure 9. Resonance contributors of the T-Hg^{II}-T pair. (**a**) Core resonance. (**b**) Further resonance associated with the anionic thymine **5**. The structure of **8** is the resonance hybrid (an average structure).

vibrational modes from all 'four' carbonyl groups in the T-Hg^{II}-T base pair (Figure 8).

From a Raman spectral perspective, a lowering of the wavenumber of a carbonyl stretching mode indicates a reduced bond order of the C=O bond. Hence, the resonance effect shown in Figure 9 might be responsible for this phenomenon. Within resonance contributors, the enolate-like structures **6** and **7** in Figure 9 would be responsible for the reduced bond order. As a result, all the resonance effects shown in Figure 9 give the resonance hybrid **8** an average structure. This interpretation is consistent with the observation of the Raman band around 1588 cm^{-1} for the TpT at pH 12.4, which originates from the deprotonated thymine base at N3 and the resulting enolate-like structure of the thymine bases (Supplementary Figure S8).

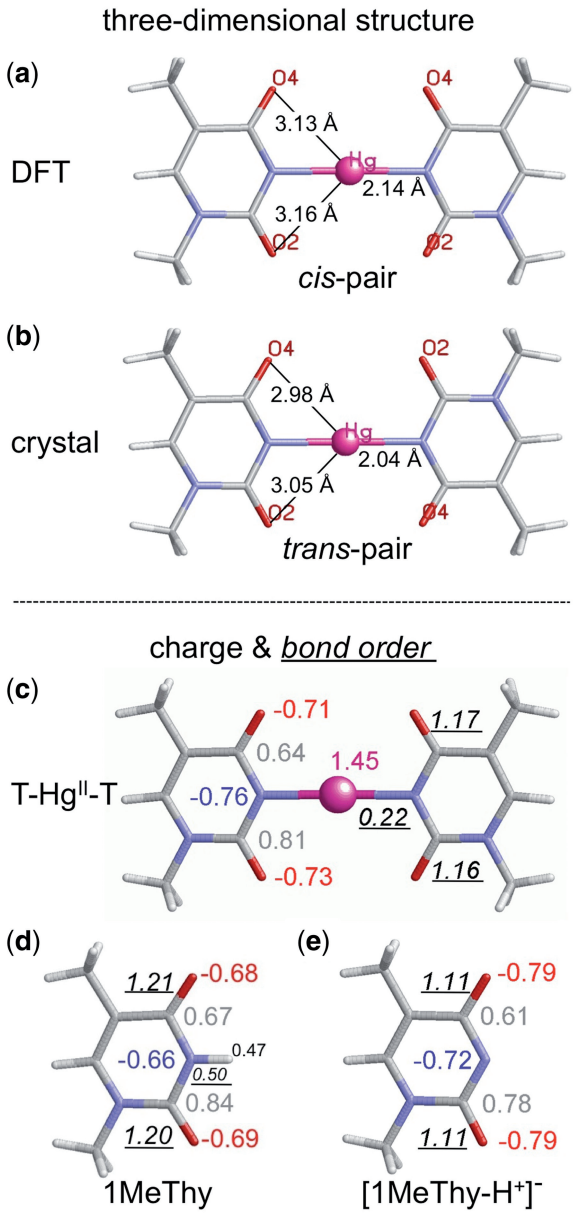

Figure 10. Results of the DFT calculations. (**a**) Key inter-atomic distances within the 1-methylthymine–Hg^{II} (2:1) complex. (**b**) Key inter-atomic distances within the crystal structure of the 1-methylthymine–Hg^{II} (2:1) complex (43). Natural charges and bond orders of (**c**) the T-Hg^{II}-T pair, (**d**) 1-methylthymine: 1MeThy and (**e**) deprotonated 1-methylthymine: [1MeThy-H$^+$]$^-$.

In addition, the same resonance effect should also reduce the effective bond order of the N-Hg^{II} bond, because in the idealized resonance contributors **2–4**, the N-Hg^{II} bond is dissociated which makes the character of the N-Hg^{II} bond ionic and weaker. The N-Hg^{II} bond is thermally cleavable even below 100°C (Supplementary Figures S3), which is indicative of an ionic character. This interpretation is consistent with our previous ^{15}N-NMR study of T-Hg^{II}-T pairs. In that study, large down-field shifts of the ^{15}N resonances of N3 were observed upon the complexation of thymine with Hg^{II} (20–22), and this chemical shift change was explained by the (partially) ionic character of the N-Hg^{II} bond, based on the theory of ^{15}N chemical shifts (21,22,54,55). However, the N-Hg^{II} bond is formally a covalent bond and, therefore, we have demonstrated that the N-Hg^{II} bonds in the T-Hg^{II}-T pair are labile covalent bonds with a significant degree of ionic character.

Next, we considered if there was any relationship between the ionicity of the N-Hg^{II} bond and the geometry of the T-Hg^{II}-T base pair calculated by the DFT method (Figure 10). The N-Hg^{II}-N linkage in the calculated geometry was essentially linear and Hg^{II}-binding to O4 seems to be weak. The calculated inter-atomic distances between the Hg atom and the keto-oxygen atoms ranged from 3.13 Å to 3.16 Å, whereas those between Hg and N3 were 2.14 Å (Figure 10a). These structural features are consistent with those observed in the crystal structure of the 1-methylthymine-Hg^{II} complex (43) (Figure 10b), namely the inter-atomic distances N3-Hg^{II}: 2.04 Å; O4-Hg^{II}: 2.98 Å; O2-Hg^{II}: 3.05 Å. This means that Hg^{II}-binding to O4 is not necessarily required for the reduction of the C4=O4 bond order.

We further characterized the bond order and the natural charge within the T-Hg^{II}-T base pair theoretically (Figure 10c–e; Supplementary Table S1). The calculated results show that the bond order of C4=O4 for the T-Hg^{II}-T pair is reduced to 1.17, from 1.21 for a neutral 1-methylthmine base (Figure 10c and d). The bond order of the N3-Hg^{II} bond becomes 0.22, which is much less than the bond order of N3–H3 (0.50; Figure 10c and d). This is consistent with our interpretation that the N–Hg^{II} bond is less covalent and rather more ionic than N–H and N–C bonds.

Consequently, the Hg^{II} atom in the T-Hg^{II}-T pair becomes cationic with a calculated natural charge of +1.45 (Figure 10c). This cationic property seems to be related to the theoretical assumption made by Voityuk (31) that the lowest unoccupied molecular orbital (LUMO) is continuously distributed around the Hg^{II} nuclei in tandem T-Hg^{II}-T base pairs. Even the LUMO orbital in a single T-Hg^{II}-T base pair possesses the same character, giving thus good pre-requisite to overlap with the density of neighboring LUMO in a consecutive T-Hg^{II}-T step (Supplementary Figure S9). This is because the Hg^{II} nucleus is the most electro-deficient part in the T-Hg^{II}-T base pairs, and may accept an additional electron. Hence, the cationic nature of the Hg^{II} nucleus is an intrinsic property of the T-Hg^{II}-T base pair.

Thus, we realistically simulated the Raman spectra, natural charges and bond orders of the T-Hg^{II}-T pair, using a model system comprising the heavy metal of Hg^{II} (1-methylthymine-Hg^{II} (2:1) complex). It is noteworthy that a metallophilic interaction between adjacent Hg^{II} nuclei in tandem U-Hg^{II}-U pairs has been recently studied (25). In combination with the findings from other theoretical studies (31,34,48), these recently proposed interactions and characteristics might be utilized to exploit the novel properties of DNA oligomers, including metal mediated base pairs like the T-Hg^{II}-T pair.

In summary, we assigned the observed Raman band at 1586 cm^{-1} to a carbonyl stretching vibration, with the

main contribution from the C4 = O4 stretching mode. The low wavenumber shift of this carbonyl vibration, measured upon adding Hg^{II}, is associated with the reduced bond order of the C4 = O4 bond. This is due to the partial enolization of the thymine bases in the T-Hg^{II}-T base pair. This effect promotes a partial ionic character of the N–Hg^{II} bond and makes the Hg^{II} atom in the T-Hg^{II}-T base pair cationic. Based on the strong agreement between the experimental and theoretical data, we conclude that the Hg^{II} atom in the T-Hg^{II}-T base pairs is cationic, and that the Hg–N3 bond is less covalent and rather more ionic than N–H and N–C bonds.

SUPPLEMENTARY DATA

Supplementary Data are available at NAR Online: Supplementary Methods, Supplementary Table 1, Supplementary Scheme 1, Supplementary Figures 1–10 and Supplementary Reference [56].

ACKNOWLEDGMENTS

The authors thank Ms. Megumi Kudo for her assistance with the thermodynamics experiments.

FUNDING

Grant-in-Aid for Scientific Research (C) (18550146 and 20550145 to Y.T.) from the Ministry of Education, Culture, Sports, Science and Technology, Japan; Human Frontier Science Program (Young Investigator Grant to Y.T. and V.S.) from the Human Frontier Science Program Organization, France; Grant Agency of the Czech Republic (P205/10/0228 to V.S. and P208/11/0105 to P.B.); Intelligent Cosmos Foundation (to Y.T.); Daiichi-Sankyo Foundation of Life Science (to Y.T. and V.S.). Funding for open access charge: Human Frontier Science Program-Young Investigator Grant.

Conflict of interest statement. None declared.

REFERENCES

1. Meggers,E., Holland,P.L., Tolman,W.B., Romesberg,F.E. and Schultz,P.G. (2000) A novel copper-mediated DNA base pair. *J. Am. Chem. Soc.*, **122**, 10714–10715.
2. Atwell,S., Meggers,E., Spraggon,G. and Schultz,P.G. (2001) Structure of a copper-mediated base pair in DNA. *J. Am. Chem. Soc.*, **123**, 12364–12367.
3. Zimmermann,N., Meggers,E. and Schultz,P.G. (2002) A novel silver(I)-mediated DNA base pair. *J. Am. Chem. Soc.*, **124**, 13684–13685.
4. Zimmermann,N., Meggers,E. and Schultz,P.G. (2004) A second-generation copper(II)-mediated metallo-DNA-base pair. *Bioorg. Chem.*, **32**, 13–25.
5. Weizman,H. and Tor,Y. (2001) 2,2′-bipyridine ligandoside: a novel building block for modifying DNA with intra-duplex metal complexes. *J. Am. Chem. Soc.*, **123**, 3375–3376.
6. Tanaka,K. and Shionoya,M. (1999) Synthesis of a novel nucleoside for alternative DNA base pairing through metal complexation. *J. Org. Chem.*, **64**, 5002–5003.
7. Tanaka,K., Yamada,Y. and Shionoya,M. (2002) Formation of silver(I)-mediated DNA duplex and triplex through an alternative base pair of pyridine nucleobases. *J. Am. Chem. Soc.*, **124**, 8802–8803.
8. Tanaka,K., Tengeiji,A., Kato,T., Toyama,N., Shiro,M. and Shionoya,M. (2002) Efficient incorporation of a copper hydroxypyridone base pair in DNA. *J. Am. Chem. Soc.*, **124**, 12494–12498.
9. Tanaka,K., Tengeiji,A., Kato,T., Toyama,N. and Shionoya,M. (2003) A discrete self-assembled metal array in artificial DNA. *Science*, **299**, 1212–1213.
10. Switzer,C. and Shin,D. (2005) A pyrimidine-like nickel(II) DNA base pair. *Chem. Commun.*, **2005**, 1342–1344.
11. Switzer,C., Sinha,S., Kim,P.H. and Heuberger,B.D. (2005) A purine-like nickel(II) base pair for DNA. *Angew. Chem. Int. Ed.*, **44**, 1529–1532.
12. Clever,G.H., Kaul,C. and Carell,T. (2007) DNA-metal base pairs. *Angew. Chem. Int. Ed.*, **46**, 6226–6236.
13. Müller,J. (2008) Metal-ion-mediated base pairs in nucleic acids. *Eur. J. Inorg. Chem.*, **2008**, 3749–3763.
14. Johannsen,S., Korth,M.M.T., Schnabl,J. and Sigel,R.K.O. (2009) Exploring metal ion coordination to nucleic acids by NMR. *Chimia*, **63**, 146–152.
15. Johannsen,S., Megger,N., Böhme,D., Sigel,R.K.O. and Müller,J. (2010) Solution structure of a DNA double helix with consecutive metal-mediated base pairs. *Nat. Chem.*, **2**, 229–234.
16. Ono,A. and Togashi,H. (2004) Highly selective oligonucleotide-based sensor for mercury(II) in aqueous solutions. *Angew. Chem. Int. Ed.*, **43**, 4300–4302.
17. Miyake,Y. and Ono,A. (2005) Fluorescent sensor for redox environment: a redox controlled molecular device based on the reversible mercury mediated folded structure formation of oligothymidylate. *Tetrahedron Lett.*, **46**, 2441–2443.
18. Miyake,Y., Togashi,H., Tashiro,M., Yamaguchi,H., Oda,S., Kudo,M., Tanaka,Y., Kondo,Y., Sawa,R., Fujimoto,T. *et al.* (2006) Mercury(II)-mediated formation of thymine-Hg^{II}-thymine base pairs in DNA duplexes. *J. Am. Chem. Soc.*, **128**, 2172–2173.
19. Tanaka,Y., Yamaguchi,H., Oda,S., Nomura,M., Kojima,C., Kondo,Y. and Ono,A. (2006) NMR spectroscopic study of a DNA duplex with mercury-mediated T-T base pairs. *Nucleosides Nucleotides Nucleic Acids*, **25**, 613–624.
20. Tanaka,Y., Oda,S., Yamaguchi,H., Kondo,Y., Kojima,C. and Ono,A. (2007) ^{15}N-^{15}N *J*-coupling across Hg^{II}: Direct observation of Hg^{II}-mediated T-T base pairs in a DNA duplex. *J. Am. Chem. Soc.*, **129**, 244–245.
21. Tanaka,Y. and Ono,A. (2008) Nitrogen-15 NMR spectroscopy of N-metallated nucleic acids: insights into ^{15}N NMR parameters and N-metal bonds. *Dalton Trans.*, **2008**, 4965–4974.
22. Tanaka,Y. and Ono,A. (2009) Structural Studies on MercuryII-mediated T-T Base-pair with NMR Spectroscopy. In: Hadjiliadis,N. and Sletten,E. (eds), *Metal Complexes—DNA Interactions*. Wiley, West Sussex, UK.
23. Johannsen,S., Paulus,S., Düpre,N., Müller,J. and Sigel,R.K.O. (2008) Using in vitro transcription to construct scaffolds for one-dimensional arrays of mercuric ions. *J. Inorg. Biochem.*, **102**, 1141–1151.
24. Kozasa,T., Miyakawa,Y., Ono,A. and Torigoe,H. (2008) The specific interaction between metal cation and mismatch base pair in duplex RNA. *Nucleic Acids Symp. Ser.*, **52**, 197–198.
25. Benda,L., Straka,M., Tanaka,Y. and Sychrovský,V. (2011) On the role of mercury in the non-covalent stabilisation of consecutive U-Hg^{II}-U metal-mediated nucleic acid base pairs: metallophilic attraction enters the world of nucleic acids. *Phys. Chem. Chem. Phys.*, **13**, 100–103.
26. Wang,Z., Zhang,D.Q. and Zhu,D.B. (2005) A sensitive and selective "turn on" fluorescent chemosensor for Hg(II) ion based on a new pyrene-thymine dyad. *Anal. Chim. Acta*, **549**, 10–13.
27. Tang,Y.L., He,F., Yu,M.H., Feng,F.D., An,L.L., Sun,H., Wang,S., Li,Y.L. and Zhu,D.B. (2006) A reversible and highly selective fluorescent sensor for mercury(II) using poly (thiophene)s that contain thymine moieties. *Macromol. Rapid Commun.*, **27**, 389–392.
28. Lee,J.S., Han,M.S. and Mirkin,C.A. (2007) Colorimetric detection of mercuric ion (Hg^{2+}) in aqueous media using DNA-functionalized gold nanoparticles. *Angew. Chem. Int. Ed. Engl.*, **46**, 4093–4096.

29. Liu,J. and Lu,Y. (2007) Rational design of "turn-on" allosteric DNAzyme catalytic beacons for aqueous mercury ions with ultrahigh sensitivity and selectivity. *Angew. Chem. Int. Ed. Engl.*, **46**, 7587–7590.
30. Wang,Z., Heon Lee,J. and Lu,Y. (2008) Highly sensitive "turn-on" fluorescent sensor for Hg^{2+} in aqueous solution based on structure-switching DNA. *Chem. Commun.*, **2008**, 6005–6007.
31. Voityuk,A.A. (2006) Electronic Coupling Mediated by Stacked [Thymine-Hg-Thymine] Base Pairs. *J. Phys. Chem. B*, **110**, 21010–21013.
32. Joseph,J. and Schuster,G.B. (2007) Long-distance radical cation hopping in DNA: the effect of thymine-Hg(II)-thymine base pairs. *Org. Lett.*, **9**, 1843–1846.
33. Ito,T., Nikaido,G. and Nishimoto,S. (2007) Effects of metal binding to mismatched base pairs on DNA-mediated charge transfer. *J. Inorg. Biochem.*, **101**, 1090–1093.
34. Bagno,A. and Saielli,G.J. (2007) Metal-mediated *J*-coupling in DNA base pairs: Relativistic DFT predictions. *J. Am. Chem. Soc.*, **129**, 11360–11361.
35. Katz,S. (1952) The reversible reaction of sodium thymonucleate and mercuric chloride. *J. Am. Chem. Soc.*, **74**, 2238–2245.
36. Thomas,C.A. (1954) The interaction of $HgCl_2$ with sodium thymonucleate. *J. Am. Chem. Soc.*, **76**, 6032–6034.
37. Dove,W.F. and Yamane,T. (1960) The complete retention of transforming activity after reversal of the interaction of DNA with mercuric ion. *Biochem. Biophys. Res. Commun.*, **1960**, 608–612.
38. Yamane,T. and Davidson,N. (1961) On the complexing of desoxyribonucleic acid (DNA) by mercuric ion. *J. Am. Chem. Soc.*, **83**, 2599–2607.
39. Katz,S. (1963) Reaction of Hg(II) and double-stranded polynucleotides a step-function theory and its significance. *Biochim. Biophys. Acta*, **68**, 240–253.
40. Eichhorn,G.L. and Clark,P. (1963) Reaction of mercury(II) with nucleosides. *J. Am. Chem. Soc.*, **85**, 4020–4025.
41. Simpson,R.B. (1964) Association constants of methylmercuric+ mercuric ions with nucleosides. *J. Am. Chem. Soc.*, **86**, 2059–2065.
42. Carrabine,J.A. (1974) Stereochemistry of nucleic acids and their constituents. 16. Mercury binding to nucleic acids—crystal and molecular structures of 2:1 complexes of uracil-mercuric chloride and dihydrouracil-mercuric chloride. *Biochemistry*, **10**, 292–299.
43. Kosturko,L.D., Folzer,C. and Stewart,R.F. (1974) Crystal and molecular-structure of a 2:1 complex of 1-methylthymine-mercury(II). *Biochemistry*, **13**, 3949–3952.
44. Mansy,S. and Tobias,R.S. (1975) Heavy metal-nucleotide reactions 4. Nature of reaction between mercury(ii) and uridine or thymidine—vibrational spectroscopic studies on binding to N(3), C(4)=O, and C(5) of uracil base. *Inorg. Chem.*, **14**, 287–291.
45. Buncel,E., Boone,C., Joly,H., Kumar,R. and Norris,A.R. (1985) Metal ion-biomolecule interactions. Part 12. 1H and 13C NMR evidence for the preferred reaction of thymidine over guanosine in exchange and competition reactions with mercury(II) and methylmercury(II). *J. Inorg. Biochem.*, **25**, 61–73.
46. Gruenwedel,D.W., Cruikshank,M.K. and Smith,G.M. (1993) Effect of Hg(II) on $d(GCGCATATGCGC)_2$ conformation - UV absorption and circular-dichroism studies. *J. Inorg. Biochem.*, **52**, 251–261.
47. Kuklenyik,Z. and Marzilli,L.G. (1996) Site-selective binding to a DNA hairpin. relationship of sequence-dependent intra- and interstrand cross-linking to the hairpin-duplex conformational transition. *Inorg. Chem.*, **35**, 5654–5662.
48. Morzyk-Ociepa,B. and Michalska,D. (2001) Vibrational spectra of 1-methylthyminate complexes with mercury(II) and potassium and ab initio calculations of the 1-MeT anion. *J. Mol. Struct.*, **598**, 133–144.
49. Frisch,M.J., Trucks,G.W., Schlegel,H.B., Scuseria,G.E., Robb,M.A., Cheeseman,J.R., Montgomery,J.A. Jr, Vreven,T., Kudin,K.N., Burant,J.C. *et al.* (2009), Gaussian 09, Revision A.02; Gaussian, Inc.: Wallingford CT.
50. Polavarapu,P.L. (1998) *Vibrational Spectra: Principles and Applications with Emphasis on Optical Activity*. Elsevier, Amsterdam, pp. 193–405.
51. Buděšínský,M., Daněček,P., Bednárová,L., Kapitán,J., Baumruk,V. and Bouř,P. (2008) Comparison of quantitative conformer analyses by nuclear magnetic resonance and Raman optical activity spectra for model dipeptides. *J. Phys. Chem. A*, **112**, 8633–8640.
52. Szczepaniak,K., Szczesniak,M.M. and Person,W.B. (2000) Raman and infrared spectra of thymine. A matrix isolation and DFT study. *J. Phys. Chem. A*, **104**, 3852–3863.
53. Morzyk-Ociepa,B., Nowak,M.J. and Michalska,D. (2004) Vibrational spectra of 1-methylthymine: matrix isolation, solid state and theoretical studies. *Spectrochim. Acta A*, **60**, 2113–2123.
54. Levy,G.C. and Lichiter,R.L. (1979) *Nitrogen-15 Nuclear Magnetic Resonance Spectroscopy*. Wiley, New York.
55. de Dios,A.C. (1996) Ab initio calculations of the NMR chemical shift. *Prog. Nucl. Magn. Reson. Spectr.*, **29**, 229–278.
56. Sklenář,V., Piotto,M., Leppik,R. and Saudek,V. (1993) Gradient-tailored water suppression for 1H-15N HSQC experiments optimized to retain full sensitivity. *J. Magn. Reson. A*, **102**, 241–245.